

## Energy Levels in $^{239}\text{Pu}$ Populated by Electron-Capture Decay of 11.9-h $^{239}\text{Am}$

F. T. Porter, I. Ahmad, M. S. Freedman, R. F. Barnes, R. K. Sjoblom,  
F. Wagner, Jr., and P. R. Fields

Chemistry Division, Argonne National Laboratory, Argonne, Illinois 60439

(Received 21 January 1972)

$\gamma$  singles spectra of mass-separated  $^{239}\text{Am}$  (11.9  $\pm$  0.1 h) samples have been measured with high-resolution Ge(Li) detectors. Conversion-electron spectra were measured at 0.1% resolution with a magnetic spectrometer and also with a cooled Si(Li) detector. An M1 multipolarity was found for the weak 124.42-keV transition from the previously known 511.84-keV state to the  $\frac{3}{2}^+$  level at 387.42 keV. The 511.84-keV state in  $^{239}\text{Pu}$  is therefore designated as the spin- $\frac{7}{2}$  member of the  $\frac{7}{2}^+(624)$  Nilsson state. New very weak intraband transitions (101.96 keV,  $E2$  and 57.3 keV, predominantly M1) depopulating the  $\frac{3}{2}^+$  state at 387.42 keV support its spin assignment. Atomic electron binding energies for the  $K$ ,  $N_{1-4}$ ,  $O_2$ , and  $O_3$  shells in Pu were obtained; small revisions in best values for Pu electron binding energies are suggested.  $\log ft$  values for the electron-capture transitions  $^{239}\text{Am} \rightarrow ^{239}\text{Pu}$  were derived.

### I. INTRODUCTION

The conversion electrons associated with the electron-capture (E.C.) decay of  $^{239}\text{Am}$  ( $t_{1/2} = 11.9$  h) were first investigated by Smith, Gibson, and Hollander (SGH)<sup>1</sup> and the  $\gamma$  rays were studied by Glass, Carr, and Gibson (GCG).<sup>2</sup> The E.C. decay of  $^{239}\text{Am}$  populates levels in  $^{239}\text{Pu}$  which are also populated by the  $\beta^-$  decay of  $^{239}\text{Np}$  and  $\alpha$  decay of  $^{243}\text{Cm}$ . The  $\beta^-$  decay<sup>3, 4</sup> of  $^{239}\text{Np}$  and  $\alpha$  decay<sup>5, 6</sup> of  $^{243}\text{Cm}$  have already been extensively investigated. From these studies rotational bands built on  $\frac{1}{2}^+(631)$ ,  $\frac{5}{2}^+(622)$ , and  $\frac{7}{2}^-(743)$  intrinsic states have been well established. The intrinsic states are described in terms of  $K\pi(Nn_z\Lambda)$  where  $K$  is the projection of the spin on the nuclear symmetry axis,  $\pi$  is the parity, and  $N$ ,  $n_z$ , and  $\Lambda$  are the asymptotic quantum numbers.<sup>7</sup> More recently levels have been identified belonging to the  $\frac{1}{2}^-(501)$  band<sup>8</sup> with band head at 469.8 keV. However, a level at 511.8 keV which is more strongly populated in  $^{239}\text{Am}$  decay has not been well characterized. (See Sec. IV for decay scheme.) The present investigation was undertaken with the aim of determining the spin of the 511.8-keV state and the reduced E.C. half-lives to various Nilsson states.<sup>7</sup>

### II. SOURCE PREPARATION

The  $^{239}\text{Am}$  samples for the present measurements were prepared by irradiating ~60 mg of  $^{237}\text{Np}$  with 30-MeV  $\alpha$  particles in the Argonne 60-in. cyclotron. The irradiation time varied from 6 to 10 h and the average  $\alpha$ -particle beam current density was 30  $\mu\text{A}/\text{cm}^2$ . The irradiated Np was dissolved by heating it with  $\text{HNO}_3$  and  $\text{HF}$ . After boiling off the  $\text{HF}$ , the material was evaporated to

dryness in *aqua regia*. The residue was then dissolved in 1 ml of 9 M HCl and the Np was extracted four successive times with equal volumes of 0.4 F Aliquat-336 in xylene. To the aqueous phase, which contained Am, 1 mg of lanthanum carrier was added and precipitated as hydroxide. The precipitate was then dissolved in a minimum amount of HCl and evaporated to dryness. The residue was then dissolved in 3 M  $\text{NH}_4\text{SCN}$ -0.01 M  $\text{H}_2\text{SO}_4$  and loaded onto a 2-mm  $\times$  6-cm column containing Aliquat-336 chloride adsorbed on hydrophobic diatomaceous earth.<sup>9, 10</sup> A solution of 1 M  $\text{NH}_4\text{SCN}$ -0.01 M  $\text{H}_2\text{SO}_4$  was then passed through the column, which removed most of the fission products. The Am was then eluted with 0.02 M  $\text{H}_2\text{SO}_4$  solution and was loaded onto another column containing di-2-ethylhexylphosphoric acid (HDEHP) adsorbed on hydrophobic diatomaceous earth.<sup>11</sup> This column was operated at 60°C. A 0.1 M HCl solution was passed through the column which removed most of the remaining fission products. The Am was then eluted with 0.5 M HCl solution. All sources of  $^{239}\text{Am}$  were deposited using the Argonne isotope separator.

### III. EXPERIMENTAL DATA

#### A. $\gamma$ -Ray Spectroscopy

Several  $\gamma$ -singles spectra of mass-separated  $^{239}\text{Am}$  samples were measured with a 1-cm<sup>3</sup> planar Ge(Li) detector and a 25-cm<sup>3</sup> coaxial Ge(Li) detector. The 1-cm<sup>3</sup> Ge(Li) spectrometer had a thin Be window and had a resolution full width at half maximum (FWHM) of 0.7 keV at 100-keV  $\gamma$ -ray energy. Figure 1 shows the  $\gamma$ -ray spectrum measured with the 1-cm<sup>3</sup> Ge(Li) spectrometer. The 124.4-keV  $\gamma$  ray in the spectrum has not been observed in the decay of  $^{239}\text{Np}$  and  $^{243}\text{Cm}$ .

The energies and intensities of higher-energy  $\gamma$  rays were measured with the 25-cm<sup>3</sup> Ge(Li) detector. A set of absorbers (0.7 g/cm<sup>2</sup> Pb, 1.1 g/cm<sup>2</sup> Cd, 0.7 g/cm<sup>2</sup> Cu, and 0.4 g/cm<sup>2</sup> Al) was used to absorb lower-energy  $\gamma$  rays and  $K$  x rays in order to reduce summing-effect interference. The spectrum thus measured is shown in Fig. 2.

The energies and intensities measured from several spectra are summarized in Table I. Intensities are expressed in percent per  $^{239}\text{Am}$  E.C. decay. These were obtained by equating the total  $\gamma$ -ray and conversion-electron intensities populating the ground-state band to 90%. A 10% E.C. feed was assigned to the ground-state band, on the

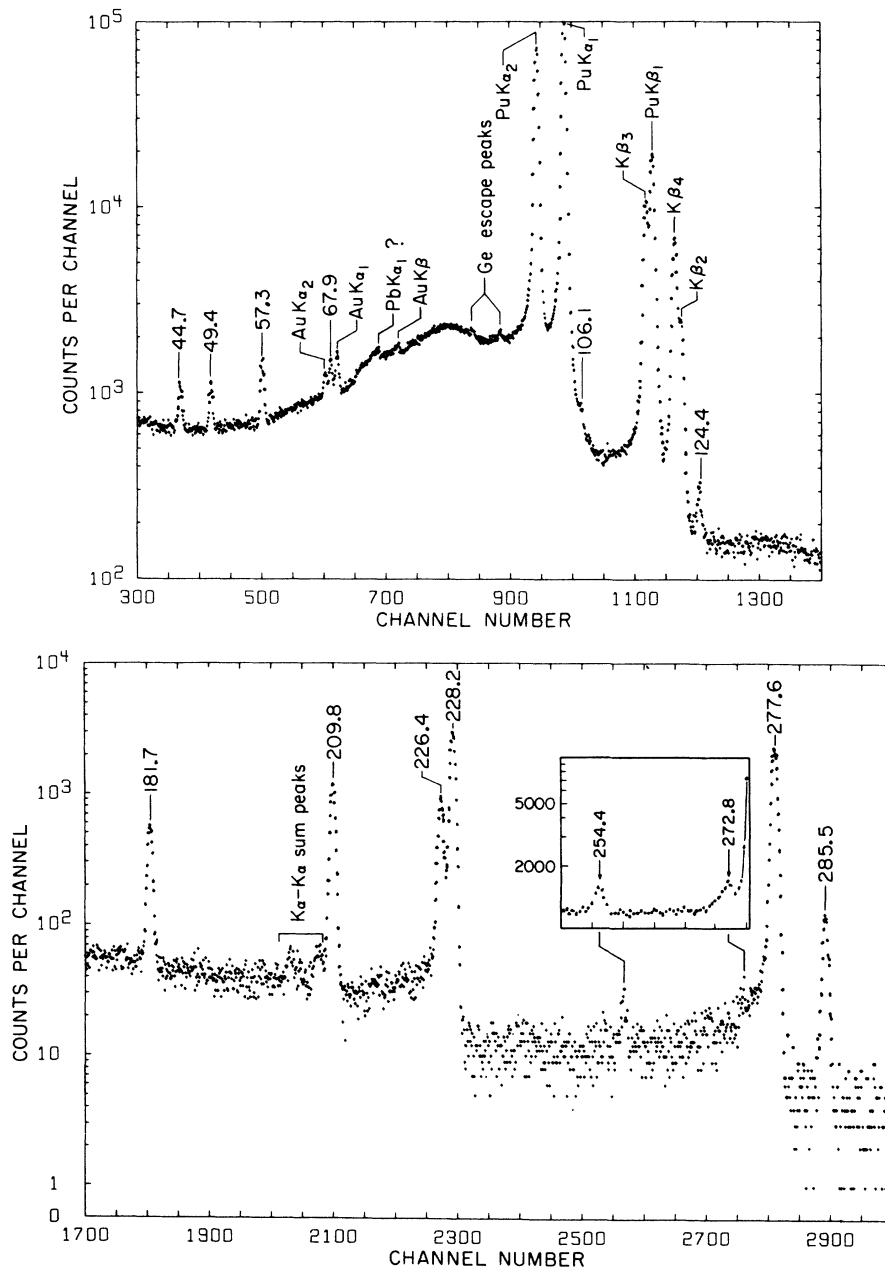


FIG. 1.  $^{239}\text{Am}$   $\gamma$ -ray spectrum measured with a 2-cm<sup>2</sup>  $\times$  0.5-cm Ge(Li) detector. The source was placed 3 cm from the detector endcap, and a 350-mg/cm<sup>2</sup> Al absorber was used to reduce Pu  $L$  x rays. Energies are given in keV. Au  $K$  x-rays originate from fluorescence of the gold electrode on the detector, and Pb x rays from shielding. Inset shows the region of the 254.4- and 272.8-keV transitions as recorded from the larger 25-cm<sup>3</sup> Ge(Li) spectrometer.

basis of evidence presented in Sec. III C and IV B.

### B. Magnetic Electron Spectroscopy

Internal-conversion electrons following the decay of  $^{239}\text{Am}$  have been surveyed by SGH<sup>1</sup> using a spectrometer with photographic-plate detector. They noted the absence of the 61.5- and 106.1-keV transitions which are evident in the  $^{239}\text{Np}$  decay to  $^{239}\text{Pu}$  levels, but found 10 transitions which had previously been seen in the  $^{239}\text{Np}$  decay.<sup>3</sup> Our efforts here were to establish some of the weaker decay routes of  $^{239}\text{Am}$ . Because of the short half-life we chose to examine only lines critical to the establishment of relative intensity differences in the decay of  $^{239}\text{Am}$  and  $^{239}\text{Np}$ , and to rely on the relative shell conversion intensities for specific transitions already well determined by Ewan, Geiger, Graham, and MacKenzie (EGGM)<sup>4</sup> in the decay of  $^{239}\text{Np}$ .

#### 1. Instrumentation

Source material was deposited on a 5-mg/cm<sup>2</sup> Al foil as 200-eV  $^{239}\text{Am}$  ions from the decelerated beam of the Argonne electromagnetic mass separator. The beam was decelerated to reduce penetration of the ions into the Al backing. Our experience shows that a source prepared with 200-V ions has very little line broadening above 20-keV electron energy for 0.1% resolution. A mask with a 3-mm-diam hole was used but the focusing was good enough to concentrate the mass in a small spot of 1–2-mm diam. Such a source in the Argonne toroidal-field spectrometers<sup>12</sup> operated in tandem with a 3-mm exit aperture yields a line width (FWHM, momentum) of  $\sim 0.11\%$  and a transmission of  $\sim 10\%$  of  $4\pi$ . Source strength was  $\sim 4 \times 10^6$  disintegrations/min; the source was completely invisible. The thickness was  $< 4 \mu\text{g}/\text{cm}^2$ .

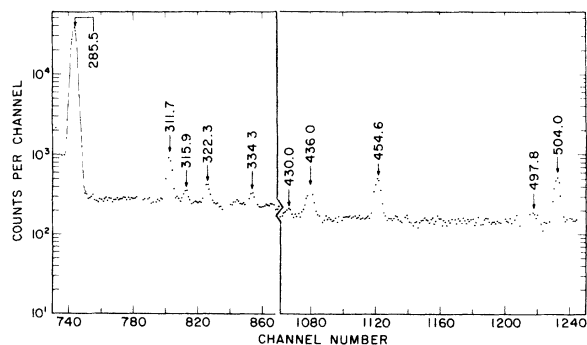


FIG. 2. High-energy portion of  $^{239}\text{Am}$   $\gamma$ -ray spectrum measured with a 25-cm<sup>3</sup> Ge(Li) spectrometer. A set of Pb, Cd, Cu, and Al absorbers was used to absorb the lower-energy  $\gamma$  rays and  $K$  x rays. Energies given in keV.

as estimated from the upper limit on background beam current and collection time in the isotope separator.

The detector was a bare cleaved-surface NaI(Tl) crystal scintillation counter whose efficiency was determined by pulse-height analysis at several energies in the range of interest. At 7.3 keV the efficiency is 65%; at 14 keV, 75%; and at 100 keV, 91%. We assign  $\sim 10\%$  uncertainty to the counter-efficiency correction in the range of 5–15 keV. A greater uncertainty in low-energy line intensities originates in energy-loss phenomena in the source material evidenced by a tail on the low-energy side of the line. The area under the tail, the extent of which is the source of the uncertainty, must be included in the line area; this area is proportional to the electron intensity.

We find it useful to plot the ratio of line area to peak height as a function of electron energy to aid in the intensity determination of weaker and not well-resolved lines. Separate curves are generated for  $K$  and for  $L, M, \dots$  conversion lines at energies where the natural width of the  $K$  level (115 eV<sup>13</sup> compared with 5–15 eV for  $L$  and  $M$  lines) becomes a significant fraction of the instrumental resolution. In addition, we find that the

TABLE I.  $^{239}\text{Am}$   $\gamma$  rays and  $K$  x rays.

Energy (keV)	Photon intensity (% per decay)	Transition (initial $\rightarrow$ final level) (keV)
44.7 $\pm$ 0.1	(9 $\pm$ 1) $\times 10^{-2}$	330.1 $\rightarrow$ 285.5
49.4 $\pm$ 0.1	0.11 $\pm$ 0.01	57.27 $\rightarrow$ 7.86
57.3 $\pm$ 0.1	0.17 $\pm$ 0.017	57.27 $\rightarrow$ 0
67.9 $\pm$ 0.1	0.13 $\pm$ 0.013	75.70 $\rightarrow$ 7.86
99.5 $\pm$ 0.1	35.0 $\pm$ 1.5	Pu $K\alpha_2$
103.8 $\pm$ 0.1	53.9 $\pm$ 2.3	Pu $K\alpha_1$
106.1 $\pm$ 0.2	(5 $\pm$ 1) $\times 10^{-2}$	391.6 $\rightarrow$ 285.5
117.1 $\pm$ 0.1	20.1 $\pm$ 1.1	Pu $K\beta_1$
120.6 $\pm$ 0.1	6.9 $\pm$ 0.4	Pu $K\beta_2$
124.4 $\pm$ 0.1	0.1 $\pm$ 0.01	511.8 $\rightarrow$ 387.4
181.7 $\pm$ 0.1	1.08 $\pm$ 0.06	511.8 $\rightarrow$ 330.1
209.8 $\pm$ 0.1	3.5 $\pm$ 0.2	285.5 $\rightarrow$ 75.70
226.4 $\pm$ 0.1	3.3 $\pm$ 0.2	511.8 $\rightarrow$ 285.5
228.2 $\pm$ 0.1	11.3 $\pm$ 0.6	285.5 $\rightarrow$ 57.27
254.4 $\pm$ 0.1	(8.4 $\pm$ 0.6) $\times 10^{-2}$	330.1 $\rightarrow$ 75.70
272.8 $\pm$ 0.1	(6.4 $\pm$ 0.5) $\times 10^{-2}$	330.1 $\rightarrow$ 57.27
277.6 $\pm$ 0.1	15.0 $\pm$ 0.7	285.5 $\rightarrow$ 7.86
285.5 $\pm$ 0.1	0.80 $\pm$ 0.05	285.5 $\rightarrow$ 0
311.7 $\pm$ 0.2	(1.7 $\pm$ 0.15) $\times 10^{-2}$	387.4 $\rightarrow$ 75.70
315.9 $\pm$ 0.2	(1.7 $\pm$ 0.15) $\times 10^{-2}$	391.6 $\rightarrow$ 75.70
322.3 $\pm$ 0.2	(2.6 $\pm$ 0.3) $\times 10^{-3}$	330.1 $\rightarrow$ 7.86
334.3 $\pm$ 0.2	(4.2 $\pm$ 0.5) $\times 10^{-3}$	391.6 $\rightarrow$ 57.27
430.0 $\pm$ 0.3	(1.7 $\pm$ 0.3) $\times 10^{-3}$	505.7 $\rightarrow$ 75.70
436.0 $\pm$ 0.3	(8 $\pm$ 1) $\times 10^{-3}$	511.8 $\rightarrow$ 75.70
454.6 $\pm$ 0.3	(1.2 $\pm$ 0.12) $\times 10^{-2}$	511.8 $\rightarrow$ 57.27
497.8 $\pm$ 0.3	(1.5 $\pm$ 0.3) $\times 10^{-3}$	505.7 $\rightarrow$ 7.86
504.0 $\pm$ 0.3	(1.4 $\pm$ 0.14) $\times 10^{-2}$	511.8 $\rightarrow$ 7.86

*L* Auger lines have a different shape and fall on a still different curve. Line intensity (either from area measurement or by determining area from peak height as described just above) was corrected for decay and counter efficiency.

Energy calibration was derived from the *K* conversion line of the 122.060-keV transition<sup>14</sup> in  $^{57}\text{Fe}$ . Line positions were determined from the medians of the upper quarter of the peaks.

## 2. Electron Binding Energies

Table II gives the binding energies in Pu used in the present work. They represent values selected from smooth curves (modified "Moseley" plots)<sup>15</sup> which are fitted to the experimental data available in the actinides<sup>16-23</sup> from  $Z=92$  to 100 and from this work. For comparison, the values of the Bearden and Burr<sup>16</sup> compilation are tabulated; many of these exhibit deviations of several probable errors from the expected smooth  $Z$  dependence.<sup>15</sup> We present our selected values for general utility, primarily because of these large deviations. The Pu binding energies determined

by EGM<sup>4</sup> were not included because they are systematically larger by 30–60 eV due to an instrumental problem the possibility of which was anticipated by their assigning errors of that magnitude.

The present work makes some contribution to the binding energy data in the following way. The energy difference between lines from the same shell of the 49.4- and the 57.3-keV transitions gives the energy of the 7.86-keV transition. From the weighted average of the  $L_1$ ,  $L_2$ ,  $L_3$ ,  $M_2$ , and  $M_3$  line-pair differences of these transitions we obtain  $7860 \pm 3$  eV for the energy of the first excited state in  $^{239}\text{Pu}$ . This enables us to calculate the  $N_{1-4}$  and  $O_{2,3}$  binding energies from the measured line energies of the 7.86-keV transition given in Table III. In addition, the *K* binding energy can be based on the  $L_1$ ,  $L_2$ , and  $M_1$  binding energies and the corresponding conversion lines of the 102- and 124-keV transitions; the sum of these energies yields the 226-keV transition energy. Our result, from the 226-keV *K* line (see Table II) is in good agreement with the more precise *K* bind-

TABLE II. Atomic electron binding energies ( $Z=94$ ) to the Fermi level of solid plutonium oxide, all values in keV  $\pm$  (eV).

Shell	Selected values <sup>a</sup>	Present work	Bearden and Burr <sup>b</sup>
<i>K</i>	121.803 (7) <sup>c</sup>	121.801 (23)	121.818 (66)
$L_1$	23.102 (5)		23.097 (2.5)
$L_2$	22.269 (3)		22.266 (1)
$L_3$	18.057 (2)		18.056 (1)
$M_1$	5.930 (3)		5.933 (2)
$M_2$	5.548 (5)		5.541 (2.5)
$M_3$	4.563 (5)		4.557 (2)
$M_4$	3.970 (4)		3.973 (1)
$M_5$	3.778 (4)		3.778 (1)
$N_1$	1.564 (4)	1.563 (4)	1.559 (1)
$N_2$	1.387 (4)	1.387 (4)	1.372 (3)
$N_3$	1.126 (2)	1.128 (4)	1.115 (2.5)
$N_4$	0.850 (1)	0.846 (8)	0.849 (1)
$N_5$	0.801 (1)		0.801 (1)
$N_6$	0.445 (10)		0.445 (2.5)
$N_7$	0.433 (10)		0.432 (3)
$O_1$	0.354 (3)		0.352 (3.5)
$O_2$	0.285 (6)	0.293 (5)	0.274 (7)
$O_3$	0.213 (6)	0.221 (4)	0.207 (7)
$O_4$	0.116 (3)		0.116 (2)
$O_5$	0.106 (3)		0.105 (1.5)
$P_1$	0.075 (10)		
$P_2$	0.040 (10)		
$P_3$	0.030 (10)		

<sup>a</sup> These values selected on the basis of smooth fits to "modified Moseley plots" of experimental binding energies vs  $Z$  in the actinides from  $Z=92$  to 100. The errors indicated are intended to be standard deviations and reflect the uncertainty in the fitting. The data were taken from Refs. 16–23 and the present work.

<sup>b</sup> Reference 16. The error values given here are standard errors adjusted from the probable errors given in Ref. 16.

<sup>c</sup> See Ref. 23 for *K* binding energy.

TABLE III. Internal-conversion lines in the decay  $^{239}\text{Am} \rightarrow ^{239}\text{Pu}$  selected for observation with magnetic spectrometer.

Transition keV $\pm$ (eV) (initial $\rightarrow$ final levels)	Shell	Electron energy keV $\pm$ (eV)	Transition energy <sup>a</sup> keV $\pm$ (eV)	Intensity <sup>b</sup>	Multipolarity: data <sup>c</sup> from which derived
7.860 (3) (7.86 $\rightarrow$ 0)	$\Sigma M$			(33.4)	99.7% M1
	$N_1$	6.297 (2)	7.861 (5)	4.00 $\pm$ 0.28	+ (0.30 $\pm$ 0.02)% E2
	$N_2$	6.473 (2)	7.860 (5)	2.92 $\pm$ 0.25	$N_1/N_2$
	$N_3$	6.732 (2)	7.858 (3)	2.86 $\pm$ 0.28	$N_1/N_3$
	$N_4$	7.014 (7)	7.864 (7)	0.08 $\pm$ 0.04	
	$N_5$	7.063 (11)	7.864 (11)	0.04 $\pm$ 0.03	
	$O_1$			(0.90)	
	$O_2$	7.567 (3)	7.852 (7)	0.69 $\pm$ 0.08	
	$O_3$	7.639 (2)	7.852 (7)	0.67 $\pm$ 0.07	
	$O_{4,5}$			(0.015)	
	$\Sigma P, Q$			(0.40)	
				46.0	
44.663 (5) (330.1 $\rightarrow$ 285.5)	$L_2$	22.394 (3)	44.663 (5)	1.35 $\pm$ 0.15	
	Other $e^-$			(10.1)	
	$\gamma$			0.09	
			11.5		
49.412 (4) (57.27 $\rightarrow$ 7.86)	$L_1$	26.304 (3)	49.406 (6)	2.20 $\pm$ 0.13	80% M1
	$L_2$	27.148 (3)	49.417 (5)	3.13 $\pm$ 0.19	+ (20 $\pm$ 2)% E2
	$L_3$	31.357 (3)	49.414 (4)	2.50 $\pm$ 0.14	$L_1/L_2$
	$M_2$	43.862 (4)	49.410 (6)	0.88 $\pm$ 0.05	$L_1/L_3$
	$M_3$	44.850 (5)	49.413 (7)	0.74 $\pm$ 0.05	
	Other $e^-$			(1.81)	
	$\gamma$			0.11	
			11.4		
57.273 (4) (57.27 $\rightarrow$ 0)	$L_1$	34.174 (4)	57.276 (6)	0.90 $\pm$ 0.05 <sup>d</sup>	E2 > 85%
	$L_2$	35.006 (4)	57.275 (5)	10.5 $\pm$ 0.5	$L_1/L_3$
	$L_3$	39.216 (4)	57.273 (4)	9.1 $\pm$ 0.5	
	$M_2$	51.723 (5)	57.271 (7)	3.19 $\pm$ 0.22	
	$M_3$	52.708 (5)	57.271 (7)	2.82 $\pm$ 0.20	
	Other $e^-$			(2.12)	
	$\gamma$			0.16	
			28.8		
67.841 (7) (75.70 $\rightarrow$ 7.86)	$L_1$	44.726 (18)	67.828 (18)	0.15 $\pm$ 0.03	E2 > 75%
	$L_2$	45.573 (5)	67.842 (7)	4.5 $\pm$ 1.0	$L_1/L_2$
	Other $e^-$			(6.0)	
	$\gamma$			0.12	
			10.8		
101.965 (13) (387.4 $\rightarrow$ 285.5)	$L_1$			$\leq$ 0.008	E2 > 80%
	$L_2$	79.701 (13)	101.970 (13)	(0.054) <sup>e</sup>	$L_1/L_3$
	$L_3$	83.888 (24)	101.945 (24)	0.034 $\pm$ 0.005	
	Other $e^-$			(0.034)	
	$\gamma$			(0.008)	
			0.13		
106.1 (391.6 $\rightarrow$ 285.5)	$L_1$			$\leq$ 0.016	
106.505 (24) (163.8 $\rightarrow$ 57.27)	$L_2$	84.236 (24)	106.505 (24)	0.048 $\pm$ 0.005	
	Other $e^-$			(0.069)	
	$\gamma$			(0.009)	
			0.126		

TABLE III (Continued)

Transition keV $\pm$ (eV) (initial $\rightarrow$ final levels)	Shell	Electron energy keV $\pm$ (eV)	Transition energy <sup>a</sup> keV $\pm$ (eV)	Intensity <sup>b</sup>	Multipolarity: data <sup>c</sup> from which derived
124.416 (15) (511.8 $\rightarrow$ 387.4)	$L_1$	101.307 (15)	124.409 (15)	$0.176 \pm 0.013$ $\leq 0.03$	$M1$ ( $E2 < 7\%$ )
	$L_2$ $M_1$ Other $e^-$ , mostly $K$ $\gamma$	118.500 (21)	124.430 (21)	$0.044 \pm 0.009$ (1.08)	$L_1/L_2$
				<u>0.10</u> 1.4	
181.715 (10) (511.8 $\rightarrow$ 330.1)	$K$	59.912 (7)	181.715 (10)	$3.1 \pm 0.6$ (0.78)	68% $M1$ + (32 $\pm$ 5)% $E2$
	Other $e^-$ $\gamma$			<u>1.08</u> 5.0	$\alpha_K$
223.6 (387.4 $\rightarrow$ 163.8)	$K$ Other $e^- + \gamma$			$\leq 0.02$ <u><math>\leq 0.02</math></u> $\leq 0.04$	
226.383 (12) (511.8 $\rightarrow$ 285.5)	$K$	104.580 (10)	226.383 (12)	$5.68 \pm 0.27$ (1.6)	77% $M1$ + (23 $\pm$ 7)% $E2$
	Other $e^-$ $\gamma$			<u>3.50</u> 10.6	$\alpha_K$
228.184 (12) (285.5 $\rightarrow$ 57.27)	$K$	106.381 (10)	228.184 (12)	$21.6 \pm 1.0$ (6.0)	88% $M1$ + (12 $\pm$ 7)% $E2$
	Other $e^-$ $\gamma$			<u>11.2</u> 38.8	$\alpha_K$
277.604 (16) (285.5 $\rightarrow$ 7.86)	$K$	155.801 (14)	227.604 (16)	$16.6 \pm 1.0$ (4.5)	88% $M1$ + (12 $\pm$ 5)% $E2$
	Other $e^-$ $\gamma$			<u>15.0</u> 36.1	$\alpha_K$
311.7 (387.4 $\rightarrow$ 75.7)	$K$			$< 0.015$	

<sup>a</sup> Calculated with selected binding energies of Table II.

<sup>b</sup> Errors include statistical, scattering-tail, and decay correction uncertainties. Error in counter-efficiency correction (uncertain by  $\sim 10\%$  between 5–15 keV; less uncertain at higher energies) not included. Units are % per  $^{239}\text{Am}$  decay assuming 10% electron capture to the ground-state band. Values in parentheses are derived quantities either from theoretical internal-conversion ratios or from experimental data of EGGM.<sup>4</sup> Transition intensities are summed.

<sup>c</sup> Theoretical internal-conversion coefficients for  $N$  and higher shells from Ref. 27, and for  $K$ ,  $L$ , and  $M$  shells from Ref. 28.

<sup>d</sup> Observed line intensity of this  $L_1$  line is composed of  $\sim$  equal contributions from the two 57.3-keV transitions. See decay scheme (Fig. 7) and text, Sec. III B 3.

<sup>e</sup> Experimental intensity of 0.086 was associated with unexplained broader line.

ing energy of Nelson, Saunders, and Salem<sup>23</sup> derived from  $K$  x-ray measurements.

### 3. Results of Electron Spectroscopy

The energies and intensities of the conversion lines observed in the present study are given in Table III. Support for the level at 387.4 comes from the very low-intensity transitions, 101.9 keV and 124.4 keV. The pertinent regions of the spec-

trum are shown in Fig. 3. It is not surprising that the 124.4–101.9-keV cascade was not seen by EGGM<sup>4</sup> in the  $^{239}\text{Np}$  decay because it constitutes only 8% of the deexcitation of the 511.8-keV level which is populated in only  $\sim 1\%$  of the  $^{239}\text{Np}$  decays, whereas the 511.8-keV level is populated in 17% of the  $^{239}\text{Am}$  decays. Further, the  $L_3$  line of the 101.9-keV transition would be completely masked by the  $L_2$  line of the 106.1-keV transition in the  $^{239}\text{Np}$  decay. The line we call  $L_3$ -101.9 cannot be

the  $L_2$ -106.1 because no  $L_1$ -106.1 is seen in  $^{239}\text{Am}$ , and EGM<sup>4</sup> have shown that  $L_1$ -106.1 and  $L_2$ -106.1 have approximately the same intensity. The line  $L_2$ -101.9 is clearly wider than normal and has ~60% too large an intensity compared to  $L_3$ -101.9 for an  $E2$  transition. Because of this unexplained contribution we calculate the intensity of the 101.9-keV transition in  $^{239}\text{Am}$  from the  $L_3$  line and the assumption that it is a pure  $E2$  as evidenced from the low  $L_1$  intensity.

The weak 124.4-keV transition is almost pure  $M1$  according to the  $L_1/L_2$  ratio and  $L_1$  conversion coefficient. In the region just below  $L_2$ -124.4 lies any possible  $K$ -223.6 (387.4 → 163.8-keV transition). Our limit is ≤0.02% per decay on the  $K$  line or ≤0.04% for the 223.6-keV transition.

The 18.429-keV transition between the 75.70- and 57.27-keV levels in the ground-state band has its conversion lines intermixed with  $L$  Auger lines. We find lines at the expected positions of the  $M_1$ ,  $M_2$ ,  $M_3$ ,  $N_1$ , and  $N_2$  lines of the 18.429-keV transition but not clearly enough resolved to say with certainty what intensity this transition has. Its total transition intensity is not more than 3% per  $^{239}\text{Am}$  decay. An intensity of ~3% would be required if our 209.8- and 67.8-keV intensities are correct.

From our selected lines of the well-established transitions the lower-energy levels of  $^{239}\text{Pu}$  involved in the  $^{239}\text{Am}$  decay can be determined within a few eV and the upper levels to ~25 eV. In the cases where redundant paths can be used to build the level energy, the agreement is consistent with the assigned errors. For example, at the 285.5-keV level, two paths, 277.6 + 7.86 and 228.2 + 57.3, yield  $285.462 \pm 0.029$  and  $285.455 \pm 0.025$  keV, respectively. Also the 511.8-keV level can be derived from either the 330-keV level plus the 181.7-keV transition or the 387.4-keV level plus the 124.4-keV transition; these yield  $511.836 \pm 0.025$  and  $511.839 \pm 0.030$  keV, respectively. We agree with EGM<sup>4</sup> (within quoted errors) on all the  $^{239}\text{Pu}$

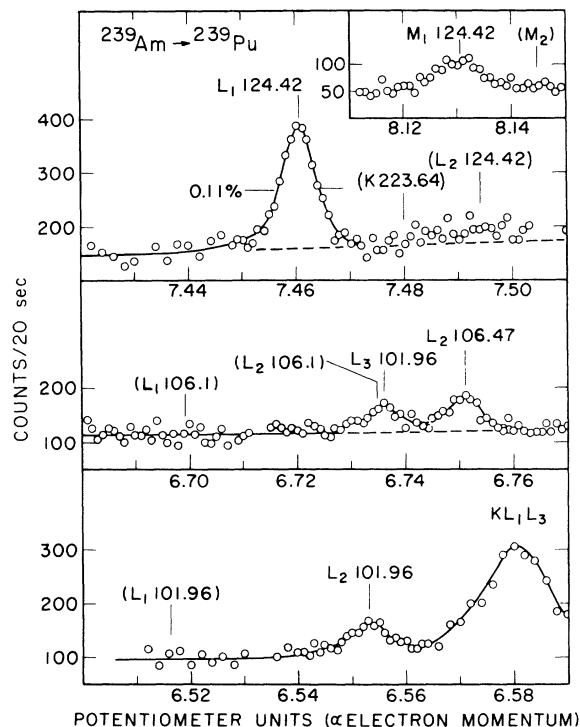


FIG. 3. Internal-conversion lines from the low-intensity 101.96- and 124.42-keV transitions in the decay of  $^{239}\text{Am} \rightarrow ^{239}\text{Pu}$ . Expected positions for various lines are indicated by vertical marks. Parentheses indicate lines for which only an upper limit on intensity was obtained. The continuum is the scattering tail of the very intense  $K$  lines of the 226.4-, 228.2-, and 277.6-keV transitions at 7.591-, 7.662-, and 9.473-potentiometer units, respectively. Note that the line labeled  $L_3$ -101.96 has little contribution from  $L_2$ -106.1 because it is known from the decay of  $^{239}\text{Np} \rightarrow ^{239}\text{Pu}$  that  $L_1$ - and  $L_2$ -106.1 have approximately equal intensity.

level energies fed by  $\beta$  decay except, of course, that we saw no electron lines from transitions involving the 391.6-keV level which is populated very weakly in  $^{239}\text{Am}$  decay.

From our level energies we predict the energy

TABLE IV. Relative (to  $L_3$  lines = 1 unit) conversion-line intensities for the 49.4- and 57.3-keV transitions following the decay of  $^{239}\text{Am}$  and  $^{239}\text{Np}$  to  $^{239}\text{Pu}$ .

Shell	57.3 keV			49.4 keV	
	$^{239}\text{Am}$ Present work	$^{239}\text{Np}$ EGM <sup>a</sup>	Pure $E2$ <sup>b</sup>	$^{239}\text{Am}$ Present work	$^{239}\text{Np}$ EGM <sup>a</sup>
$L_1$	$0.099 \pm 0.008$	$0.054 \pm 0.012$	0.048	$0.92 \pm 0.07$	$1.06 \pm 0.25$
$L_2$	$1.16 \pm 0.09$	$1.18 \pm 0.23$	1.26	$1.25 \pm 0.10$	$1.24 \pm 0.30$
$L_3$	1	1	1	1	1
$M_2$	$0.35 \pm 0.03$	$0.38 \pm 0.07$	0.34	$0.35 \pm 0.03$	$0.38 \pm 0.09$
$M_3$	$0.31 \pm 0.03$	$0.27 \pm 0.05$	0.28	$0.29 \pm 0.03$	$0.30 \pm 0.08$

<sup>a</sup> Reference 4.

<sup>b</sup> Reference 28.

of the intraband transition from the 387.4- to the 330.1-keV level to be  $57.302 \pm 0.030$  keV (we call this the upper 57-keV transition). Conversion lines from this transition would be within a line-width ( $\sim 75$  eV) of the same lines of the strong 57.273-keV transition. We note first that the upper 57 keV will probably have a large  $M1$  contribution as opposed to the pure  $E2$  character of the lower 57-keV transition, and second that in the  $^{239}\text{Np}$   $\beta$  decay the relative intensity of the upper 57-keV transition would be 10 times smaller than in  $^{239}\text{Am}$  because of the smaller population of the 387.4-keV level following the  $\beta^-$  decay. Table IV shows the line intensities of the 49.4- and 57.3-keV transitions for the  $^{239}\text{Am}$  decay from our work and for the  $^{239}\text{Np}$  decay from EGGM. It is clear that the 57.3-keV  $L_1$  line is more intense relative to the  $L_{2,3}$  and  $M_{2,3}$  lines in the  $^{239}\text{Am}$  decay. The  $L_1/L_3$  ratio of the 57.3-keV transition is a factor of 2 larger in  $^{239}\text{Am}$  than in  $^{239}\text{Np}$ , whereas all other line ratios agree to better than 15%, e.g., the 49.41-keV line ratios given in Table IV. Furthermore, the theoretical ratios for a pure  $E2$  transition agree with  $^{239}\text{Np}$  data rather than the  $^{239}\text{Am}$

data. Our interpretation is that this is evidence for the upper 57-keV transition, which has a large  $M1$  component. If it were pure  $M1$ , its intensity, calculated by assigning the 50% excess  $L_1$  intensity to it and by using theoretical conversion coefficients, is 0.7% per decay. This is a lower limit on its intensity, since a small  $E2$  admixture can contribute significantly to the upper 57.3-keV components of the  $L_2$  and  $L_3$  lines with little contribution to  $L_1$  and little fractional reduction in the lower 57.3-keV intensity. Figure 4 shows the  $L$ -subshell lines from the 57.3- and 49.4-keV transitions. The  $L_1$ -57.3 line shows no obvious broadening. Therefore, since it is composed of two approximately equal intensity components the energy of the upper 57-keV transition is within<sup>24</sup>  $\sim 10$  eV of the lower 57-keV transition, which is consistent with the prediction from the level energies.

Figure 5 shows the region of the  $N, O, \dots$  conversion lines of the 7.86-keV transition. A very similar spectrum is displayed by Ewan and Graham<sup>25</sup> for this transition populated from the  $\text{Np}^{239}$  decay. Bhalla<sup>26</sup> calculated the  $N$ -subshell ratios for this particular transition and concluded that the  $E2$  mixing was  $(0.28 \pm 0.07)\%$ . Dragoun, Pauli, and Schmutzler<sup>27</sup> have used the EGGM<sup>4, 25</sup> data with their calculated internal conversion coefficients to derive the  $E2$  mixing. Our data give the

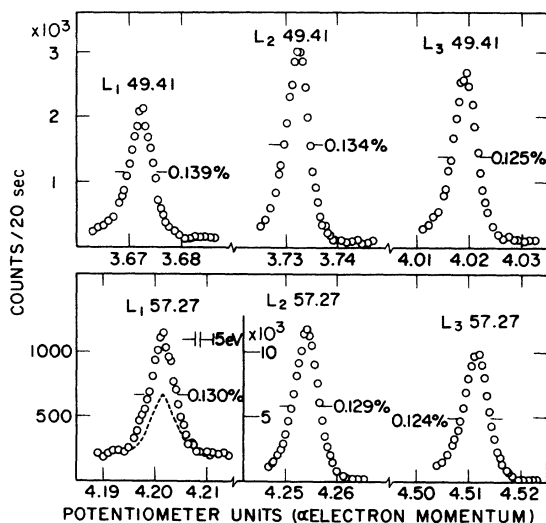


FIG. 4. The  $L$ -subshell conversion lines of the 57.27- and 49.41-keV transitions in the  $^{239}\text{Am} \rightarrow ^{239}\text{Pu}$  decay. The line  $L_1$ -57.26 is a factor of  $\sim 2$  larger than that expected for a pure  $E2$  transition (shown by dashed curve). In the  $^{239}\text{Np} \rightarrow ^{239}\text{Pu}$  decay this same transition shows an  $L_1$  intensity expected for a pure  $E2$  transition. (See Table IV.) This is interpreted as evidence for another 57.3-keV transition of predominantly  $M1$  multipolarity. This second 57.3-keV transition is indeed expected from the level scheme of  $^{239}\text{Pu}$ . Note little if any broadening due to the doublet at this resolution. The linewidth increase  $L_3 \rightarrow L_2 \rightarrow L_1$  in both the 57.26- and 49.41-keV cases is due to the progressively larger natural widths of the  $L_2$  and  $L_1$  levels.

TABLE V. Total intensity of the 7.86-keV transition based on theoretical internal-conversion coefficients normalized to the average of the experimental intensities in the  $N_{1,2,3}$  subshells. Intensities in percent per  $^{239}\text{Am}$  decay assuming 10% electron capture to the ground-state band.

Shell	Theory		Experiment
	0.997 $M1$ + 0.003 $E2$		
$M_1$	13.7		
$M_2$	9.9		
$M_3$	9.5		
$M_4$	0.17		
$M_5$	0.11		
$N_1$	4.02		$4.00 \pm 0.28$
$N_2$	2.96		$2.92 \pm 0.25$
$N_3$	2.81		$2.86 \pm 0.28$
$N_4$	0.055		$0.08 \pm 0.04$
$N_5$	0.033		$0.04 \pm 0.03$
$O_1$	0.90		
$O_2$	0.60		$0.69 \pm 0.08$
$O_3$	0.68		$0.67 \pm 0.07$
$O_4$	0.010		
$O_5$	0.005		
$P_1$	0.176		
$P_2$	0.095		
$P_3$	0.110		
$Q_1$	0.016		
	45.9		



same result, namely  $(0.30 \pm 0.02)\% E2$ .

Attempts to find the total 7.86-keV intensity and to compare it with the known population of the state by electromagnetic transitions (and thereby deduce possible electron capture to the state) are difficult not only because the  $O_1$  and  $P$  shell lines are obscured by  $L$  Auger lines but also because the  $M$  lines are too low in energy for reliable intensity measurements. We have, however, made an estimate using the calculated internal-conversion coefficients of Dragoun *et al.*<sup>27</sup> for  $N$ ,  $O$ ,  $P$ , and  $Q$  shells and the Hager and Seltzer<sup>28</sup> calculations for the  $M$  shells. We extrapolate on a log-log plot of conversion coefficient vs energy  $N$ ,  $O$ ,  $P$ , and  $Q$  and use the computer interpolation sug-

gested by Hager and Seltzer<sup>28</sup> for the  $M$  shells. Table V gives the calculated intensities for  $0.997 M1 + 0.003 E2$  normalized on the  $N_{1-3}$  average experimental intensities. The total intensity thus derived is *smaller* by  $\sim 20\%$  than the sum of the incoming transitions to the 7.86-keV state. While this discrepancy is at the limit of our experimental uncertainty concerning the intensity of the  $N$  and  $O$  lines, it is also true that no other test of the  $M/N$  conversion ratios for these calculations at such a low energy is known to us.

In Table III the intensities are given in percent per decay on the assumption that the E.C. feed to the ground-state band is 10%. The  $\gamma$  intensities and the electron intensities are related through

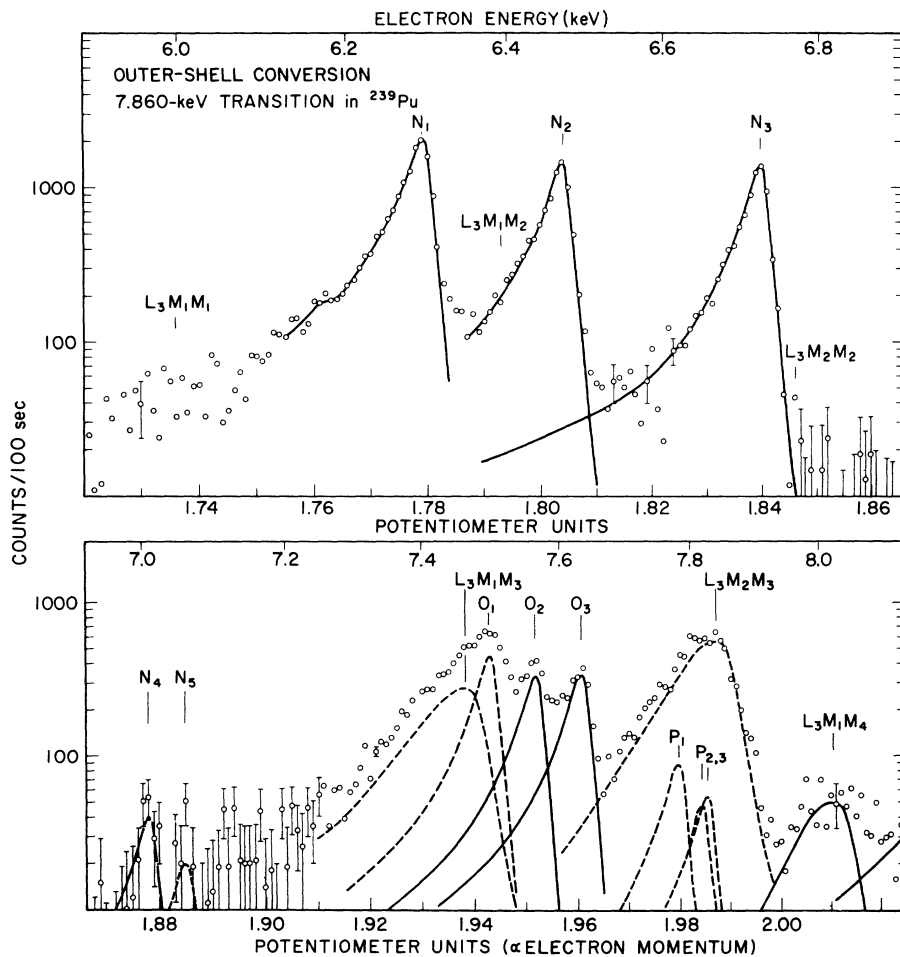


FIG. 5. Outer-shell conversion lines of the 7.860-keV transition in  $^{239}\text{Pu}$ . The abscissa is a logarithmic momentum scale. We used the  $N_3$  line shape for the analysis of the  $O$  and  $P$  lines. The dashed curves for  $O_1$ ,  $N_5$ , and  $P$  lines have the intensities predicted by theoretical conversion coefficients and by the  $M1-E2$  mixing derived from the  $N$ -subshell intensities (see Table V). All the  $L$  Auger lines expected in this region are indicated. The much broader line shape for the  $L$  Auger lines is obtained from the well-resolved  $L_3M_3M_3$  line at 8.8 keV (not shown). A background of 210 counts/100 sec has been subtracted from all data points. Possible structure on the tail of the  $N_1$  line at 1.762 potentiometer units may be due to "shakeoff" of  $O_{4,5}$  electrons accompanying  $N_1$  conversion.



feed<sup>30</sup> to these same levels of <sup>239</sup>Pu. In deducing this E.C. feed we have assumed that 5% of the 57.3-keV ( $L_1+L_2$ ) is contributed by the upper 57.3-keV transition.

#### D. Half-Life and $\alpha/(\alpha+E.C.)$ Branching Ratio

The half-life of the <sup>239</sup>Am was measured by following the decay of the 277.6-keV  $\gamma$  ray. The half-

life was found to be  $11.9 \pm 0.1$  h, in good agreement with the value ( $12.1 \pm 0.4$  h) reported by GCG.<sup>2</sup> The  $\alpha$ -particle energy of the most prominent group was measured to be  $5.772 \pm 0.005$  MeV, in agreement with the recently measured value<sup>31</sup> ( $5.776 \pm 0.002$  MeV). The  $\alpha/(\alpha+E.C.)$  ratio was determined to be  $(1.0 \pm 0.1) \times 10^{-20\%}$ , using the 277.6-keV intensity as 15 photons per 100 E.C. decays.

TABLE VI. <sup>239</sup>Am electron data obtained with the cooled Si(Li) detector.

Transition (keV)	Intensity (% per decay)	Conversion <sup>a</sup> coefficient	Multipolarity <sup>b</sup>
49.4 ( $L_1+L_2$ )	5.7	$54 \pm 5$	$M1+E2$
$L_3$	2.4	$23 \pm 2$	
$M$	2.4	$23 \pm 2$	
$N$	0.66	$6.2 \pm 0.7$	
57.3 ( $L_1+L_2$ )	11.7	$71 \pm 7$	$E2$
$L_3$	11.0	$66 \pm 6$	
$M$	6.2	$37 \pm 3$	
$N$	2.0	$12 \pm 1.2$	
67.8 ( $L_1+L_2$ )	4.8	$38 \pm 4$	$E2$
$L_3$	3.8	$30 \pm 3$	
$M$	2.1	$16.7 \pm 1.7$	
$N$	0.83	$6.5 \pm 0.7$	
181.7 $K$	3.1	$2.9 \pm 0.2$	$M1$
( $L_1+L_2$ )	0.81	$0.75 \pm 0.06$	
$M$	0.20	$0.18 \pm 0.02$	
$N$	0.063	$0.058 \pm 0.006$	
209.8 $K$	8.0	$2.3 \pm 0.15$	$M1$
$L_1+L_2$	1.7	$0.47 \pm 0.03$	
$N$	0.15	$0.043 \pm 0.004$	
226.4 $K$	5.9	$1.8 \pm 0.13$	$M1$
( $L_1+L_2$ )	1.4	$0.41 \pm 0.03$	
$M$	0.38	$0.11 \pm 0.01$	
$N$	0.14	$0.040 \pm 0.004$	
228.2 $K$	21.6	$1.9 \pm 0.12$	$M1$
$L_1+L_2$	4.5	$0.40 \pm 0.03$	
$M$	1.0	$0.09 \pm 0.01$	
$N$	0.35	$0.031 \pm 0.003$	
254.4 $K$	0.15	$1.8 \pm 0.2$	$M1$
$L_1+L_2$	0.029	$0.34 \pm 0.04$	
277.6 $K$	16.7	$1.11 \pm 0.05$	$M1$
$L_1+L_2$	3.41	$0.23 \pm 0.015$	
$L_3$	0.036	$0.0024 \pm 0.0002$	
$M$	0.86	$0.057 \pm 0.004$	
$N$	0.29	$0.019 \pm 0.002$	
285.5 $K$	0.075	$0.094 \pm 0.009$	$E2$
$L_1+L_2$	0.065	$0.08 \pm 0.008$	

<sup>a</sup> Si(Li) and Ge(Li) detector system calibrated with the 279-keV transition in Tl<sup>203</sup>;  $K$  conversion coefficient =  $0.163 \pm 0.002$ .

<sup>b</sup> The  $E2$  admixture in the lower-energy transitions is more accurately determined by the magnetic spectrometer and is given in Table III.

## IV. DISCUSSION

## A. Decay Scheme

The decay scheme of  $^{239}\text{Am}$  is shown in Fig. 7. The assignments of the ground state, 285.46-, and 391.6-keV levels to the  $\frac{1}{2}^+(631)$ ,  $\frac{5}{2}^+(622)$ , and  $\frac{7}{2}^-(743)$  Nilsson states<sup>7</sup> have been made previously from the study of the  $\beta^-$  decay<sup>3, 4</sup> of  $^{239}\text{Np}$  and  $\alpha$  decay<sup>5, 6</sup> of  $^{243}\text{Cm}$ . The ground-state spin has also been determined experimentally<sup>32</sup> to be  $\frac{1}{2}$ . The other assignments are based mainly on the measured multipolarities of the transitions originating from these levels. The results of the present investigation fully support the above assignments. From the observed energies of the members of the ground-state  $\frac{1}{2}^+(631)$  band we calculate its rotational constant,  $\hbar^2/2\mathcal{I}$ , and decoupling parameter  $a$ , as 6.251 keV and  $-0.581$ , respectively. The rotational constant of the  $\frac{5}{2}^+(622)$  band is calculated to be 6.380 keV.

The level at 511.8 keV has been found to decay to the  $\frac{5}{2}$ ,  $\frac{7}{2}$ , and  $\frac{9}{2}$  members of the  $\frac{5}{2}^+(622)$  band.

The  $M1$  multipolarities of these three transitions (226.4, 181.7, and 124.4 keV) uniquely determine the spin and parity of the 511.8-keV state as  $\frac{7}{2}^+$ . This level is therefore given an assignment of  $\frac{7}{2}^+(624)$ , which is the only  $\frac{7}{2}^+$  single-particle state expected in this energy region.

The weak 430.0- and 497.8-keV  $\gamma$  rays, as indicated in Fig. 7, originate from a level at  $505.7 \pm 0.2$  keV. This deexcitation pattern to the ground-state band is quite similar to that of a  $505.3 \pm 0.2$ -keV level populated in the  $^{239}\text{Np}$  decay,<sup>8</sup> namely, the transition to the 57.27-keV level is relatively weak compared with the transitions to the 75.70- and 7.86-keV levels. We equate these levels and use the Davies and Hollander<sup>8</sup> deduction that it is the spin- $\frac{5}{2}$  member of the  $\frac{1}{2}^-(501)$  band. There is, however, an obvious difference in the  $\beta$  decay transitions to the band from the two parent states. The  $^{239}\text{Np}$   $\beta^-$  decay favors the spin- $\frac{3}{2}$  member of the band, whereas the  $^{239}\text{Am}$  electron capture favors the spin- $\frac{5}{2}$  member.

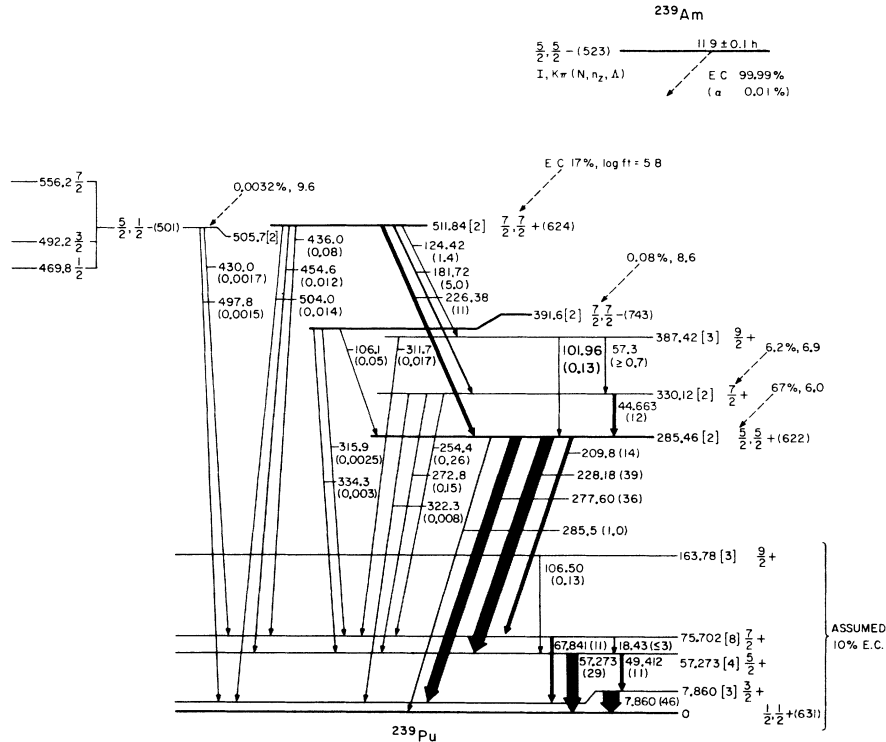


FIG. 7. Decay scheme of  $^{239}\text{Am}$  to levels in  $^{239}\text{Pu}$ . Energies are in keV. The only energy errors given here are for the level energies; the error in the last quoted figure is given in square brackets [ ]. Transition-energy errors are listed in Tables I and III. Transition intensities are given in parentheses near the transition energy, units are (percent per  $^{239}\text{Am}$  decay). The spin, parity, and quantum-number assignments for the 511.8-keV level and the multipolarities of the new low-intensity deexcitations of the 387.4-keV state are from present work. Transition intensities have errors between 10–20% plus a correlated contribution from the uncertainty in the assigned 10% electron capture to the ground-state band. At the left are other members of the  $\frac{1}{2}^-(501)$  band not observed in  $^{239}\text{Am}$  decay but seen in the decay of  $^{239}\text{Np}$  (Ref. 8).

### B. Electron-Capture Transition Probabilities

The present experiments do not yield any direct information about the E.C. feed to the  $\frac{1}{2}$  and  $\frac{3}{2}$  members of the ground-state band. However, the ratios of the 57.3-keV ( $L_1 + L_2$ ) and 277.6-keV  $K$  electron intensities in the  $^{239}\text{Np}$  and  $^{239}\text{Am}$  electron spectra indicate that the 57.3-keV level of  $^{239}\text{Pu}$  receives almost equal amounts of direct population in the decay of both nuclides. In the  $^{239}\text{Np}$  decay the  $\beta^-$  decay intensity to the ground-state band has been measured<sup>30</sup> to be 10%. We, therefore, have assigned 10% E.C. feed to the ground-state band. The E.C. feed to other levels was calculated by summing the intensities of  $\gamma$  rays and conversion electrons originating from that level. The intensities thus determined are given in Fig. 7. The  $\log ft$  values were calculated by the method of Major and Biedenharn,<sup>33</sup> using 810 keV for the  $^{239}\text{Am}$  decay energy.<sup>34</sup>

The very high  $\log ft$  value of 8.6 for the E.C. transition to the  $\frac{7}{2}^-(743)$  state at 391.6 keV clearly shows that the ground state of  $^{239}\text{Am}$  is different from that of  $^{239}\text{Np}$  (the  $\log ft$  value of  $\beta^-$  decay to this state of 6.5). The ground states of all of the known<sup>35</sup> odd-mass Am isotopes are found to be either the  $\frac{5}{2}^-(523)$  or the  $\frac{5}{2}^+(642)$  Nilsson state. Since the ground state of  $^{239}\text{Np}$  is known<sup>35</sup> to be  $\frac{5}{2}^+(642)$ , the ground state of  $^{239}\text{Am}$  should be

$\frac{5}{2}^-(523)$ . This assignment is in agreement with the assignment<sup>36</sup> made on the basis of  $\alpha$  decay of  $^{243}\text{Bk}$ .

The large retardation in the E.C. transition probability to the  $\frac{7}{2}^-(743)$  state is in agreement with the theoretical expectation. Recent calculations by Chasman<sup>37</sup> show that the  $\frac{7}{2}^-(743)$  state is 90%  $J = \frac{15}{2}$  and the  $\frac{5}{2}^-(523)$  state is 90%  $J = \frac{9}{2}$ . The mismatch between the angular momenta of the two states causes the high retardation in E.C.-decay transitions.

The total number of  $K$ -shell holes per decay can be calculated from the theoretical prediction<sup>38</sup> of  $K$ /total capture and the experimental number of  $K$  conversions per decay. For  $^{239}\text{Am}$  we find 52%  $K$  holes per decay from  $K$  conversion and 70%  $K$  holes per decay from  $K$  capture. Using a  $K$  fluorescence yield of 97%, we predict 118  $K$  x rays per 100 E.C. decays, which is in agreement with the experimental result of  $116 \pm 4$   $K$  x rays per 100  $^{239}\text{Am}$  E.C. decays. This agreement is additional support for the assignment of  $\sim 10\%$  E.C. population of the ground-state band.

### ACKNOWLEDGMENTS

The authors wish to thank J. Lerner for the isotope-separator preparation of the  $^{239}\text{Am}$  samples and R. R. Chasman for helpful discussions.

<sup>1</sup>W. G. Smith, W. M. Gibson, and J. M. Hollander, *Phys. Rev.* **105**, 1514 (1957).

<sup>2</sup>R. A. Glass, R. J. Carr, and W. M. Gibson, *J. Inorg. Nucl. Chem.* **13**, 181 (1960).

<sup>3</sup>J. M. Hollander, W. G. Smith, and J. W. Mihelich, *Phys. Rev.* **102**, 740 (1956).

<sup>4</sup>G. T. Ewan, J. S. Geiger, R. L. Graham, and D. R. MacKenzie, *Phys. Rev.* **116**, 950 (1959).

<sup>5</sup>F. Asaro, S. G. Thompson, F. S. Stephens, Jr., and I. Perlman, unpublished results cited in *The Nuclear Properties of the Heavy Elements*, edited by E. K. Hyde, I. Perlman, and G. T. Seaborg (Prentice-Hall, Englewood Cliffs, New Jersey, 1964), Vol. II, p. 892.

<sup>6</sup>B. S. Dzhelepov, R. B. Ivanov, V. G. Nedovesov, and V. P. Chechev, *Zh. Eksperim. i Teor. Fiz.* **45**, 1360 (1963) [transl.: *Soviet Phys.-JETP* **18**, 937 (1964)].

<sup>7</sup>S. G. Nilsson, *Kgl. Danske Videnskab. Selskab, Mat.-Fys. Medd.* **29**, No. 16 (1955).

<sup>8</sup>D. W. Davies and J. M. Hollander, *Nucl. Phys.* **68**, 161 (1965).

<sup>9</sup>E. P. Horwitz, L. J. Sauro, and C. A. A. Bloomquist, *J. Inorg. Nucl. Chem.* **29**, 2033 (1967).

<sup>10</sup>P. G. Barbano and L. Rigali, *J. Chromatog.* **29**, 309 (1967).

<sup>11</sup>R. J. Sochacka and S. Siekierski, *J. Chromatog.* **16**, 376 (1964).

<sup>12</sup>M. S. Freedman, F. Wagner, F. T. Porter, J. Terandy, and P. P. Day, *Nucl. Inst. Methods* **8**, 225 (1960).

<sup>13</sup>G. C. Nelson, W. John, and B. G. Saunders, *Phys. Rev.* **187**, 1 (1969).

<sup>14</sup>R. C. Greenwood, R. G. Helmer, and R. J. Gehrke [*Nucl. Instr. Methods* **77**, 141 (1969)] give  $122.061 \pm 0.010$  keV. In *Nucl. Instr. Methods* **96**, 173 (1971) the same authors give a better value of  $122.063 \pm 0.004$  keV. We have obtained  $122.057 \pm 0.005$  keV from a preliminary comparison of the  $K$  line of this transition with the  $K$  line of the 145.440  $\pm 0.003$ -keV transition [J. J. Reidy, private communication] in  $\text{Pr}^{141}$ . If we average our result with that of Helmer *et al.* we find  $122.060 \pm 0.004$  keV for the  $\gamma$  energy and an energy of  $114.939 \pm 0.005$  keV for the  $K$  line of an oxide source in the aluminum spectrometer chamber. Spectrometer work function =  $4 \pm 1$  keV,  $K$  binding energy in Fe =  $7114 \pm 2$  eV, and chemical shift =  $3.3 \pm 0.4$  eV. Constants used in converting from energy to momentum are taken from the adjustments of B. N. Taylor, W. H. Parker, and D. N. Langenberg, *Rev. Mod. Phys.* **41**, 375 (1969).

<sup>15</sup>P. Bergvall and S. Hagström, *Arkiv Fysik* **17**, 61 (1960).

<sup>16</sup>J. A. Bearden and A. F. Burr, *Rev. Mod. Phys.* **39**, 125 (1967):  $Z = 92, 93$ , and 94.

<sup>17</sup>A. Fahlman, K. Hamrin, R. Nordberg, C. Nordling, K. Siegbahn, and L. W. Holm, *Phys. Letters* **19**, 643 (1966):  $Z = 94$ .

<sup>18</sup>K. Siegbahn, C. Nordling, A. Fahlman, R. Nordberg, K. Hamrin, J. Hedman, G. Johansson, T. Bergmark,

S. -E. Karlson, and B. Lindberg, *Electron Spectroscopy for Chemical Analysis* (Almqvist and Wiksells Boktryckeri AB, Uppsala, Sweden, 1967), p. 225.

<sup>19</sup>Y. Y. Chu, M. L. Perlman, P. F. Dittner, and C. E. Bemis, Jr., *Phys. Rev. A* **5**, 67 (1972):  $Z=96$ .

<sup>20</sup>J. M. Hollander, M. D. Holtz, T. Novakov, and R. L. Graham, *Arkiv Fysik* **28**, 375 (1965):  $Z=97$ .

<sup>21</sup>I. Ahmad, F. T. Porter, M. S. Freedman, R. F. Barnes, R. K. Sjoblom, F. Wagner, Jr., J. Milsted, and P. R. Fields, *Phys. Rev. C* **3**, 390 (1971):  $Z=98$ .

<sup>22</sup>F. T. Porter and M. S. Freedman, *Phys. Rev. Letters* **27**, 293 (1971):  $Z=100$ .

<sup>23</sup>G. C. Nelson, B. G. Saunders, and S. I. Salem, *Z. Physik* **235**, 308 (1970):  $K$  binding energy  $Z=94$ .

<sup>24</sup>K. Siegbahn, C. Nordling, G. Johansson, J. Hedman, P. F. Hedén, K. Hamrin, U. Gelius, T. Bergmark, L. Werme, R. Manne, and Y. Baer, *Electron Spectroscopy for Chemical Analysis Applied to Free Molecules* (North-Holland, Amsterdam, 1969), Appendix D, p. 170: exhibits composite shapes.

<sup>25</sup>G. T. Ewan and R. L. Graham, in *Alpha-Beta- and Gamma-Ray Spectroscopy*, edited by K. Siegbahn (North-Holland, Amsterdam, 1965), p. 960.

<sup>26</sup>C. P. Bhalla, in *Nuclear Spin-Parity Assignments*, edited by N. B. Gove and R. L. Robinson (Academic, New York, 1966), p. 104.

<sup>27</sup>O. Dragoun, H. C. Pauli, and F. Schmutzler, *Nucl. Data A6*, 235 (1969); O. Dragoun, Z. Plajner, and F. Schmutzler, Max-Planck-Institut für Kernphysik, Heidelberg Report No. MPIH-1969-V5, (unpublished).

<sup>28</sup>R. S. Hager and E. C. Seltzer, *Nucl. Data A4*, 1 (1968).

<sup>29</sup>W. L. Croft, B. G. Petterson, and J. H. Hamilton, *Nucl. Phys.* **48**, 267 (1963).

<sup>30</sup>R. D. Connor and I. L. Fairweather, *Proc. Phys. Soc. (London)*, **74**, 161 (1959).

<sup>31</sup>D. J. Gorman and F. Asaro, *Phys. Rev. C* **3**, 746 (1971).

<sup>32</sup>B. Bleaney, P. M. Llewellyn, M. H. L. Pryce, and G. R. Hall, *Phil. Mag.* **45**, 773 (1954).

<sup>33</sup>J. K. Major and L. C. Biedenharn, *Rev. Mod. Phys.* **26**, 321 (1954).

<sup>34</sup>A. Artna-Cohen, *Nucl. Data*, **B6**(No. 6), 577 (1971).

<sup>35</sup>C. M. Lederer, J. M. Hollander, and I. Perlman, *Table of Isotopes* (Wiley, New York, 1967); Y. A. Ellis and A. H. Wapstra, *Nucl. Data B3*(No. 2), 1 (1969).

<sup>36</sup>I. Ahmad, Lawrence Radiation Laboratory Report No. UCRL-16888, 1966 (unpublished).

<sup>37</sup>R. R. Chasman, *Phys. Rev. C* **3**, 1803 (1971); also private communication.

<sup>38</sup>H. Brysk and M. E. Rose, presented in A. H. Wapstra, G. J. Nijgh, and R. van Lieshout, *Nuclear Spectroscopy Tables* (North-Holland, Amsterdam, 1959), p. 59.

## Properties of Levels in $^{198}\text{Pb}$ and $^{200}\text{Pb}^\dagger$

K. Krien, E. H. Spejewski,\* R. A. Naumann, and H. Hübel‡

*Joseph Henry Laboratories of Physics,  
Frick Chemical Laboratory and Princeton-Pennsylvania Accelerator,  
Princeton University, Princeton, New Jersey 08540*

(Received 13 January 1972)

The decay of  $^{198}\text{Bi}$  and  $^{200}\text{Bi}$  to levels in the corresponding Pb daughters have been investigated using sources which were both mass-separated and chemically processed.  $\gamma$ -ray and conversion-electron singles spectra were obtained, as well as  $\gamma$ - $\gamma$  prompt- and delayed-coincidence spectra. These data yield levels in  $^{198}\text{Pb}$  at the following energies (spin-parities): 1062.9 ( $2^+$ ), 1624.9 ( $4^+$ ), 1822.3 [(5) $^-$ ], and 2139.8 [(7) $^-$ ] keV. Those in  $^{200}\text{Pb}$  are at 1026.3 ( $2^+$ ), 1488.3 ( $4^+$ ), 1907.9 [(5) $^-$ ], and 2152.9 [(7) $^-$ ] keV. The half-life of the 1822-keV level in  $^{198}\text{Pb}$  was determined to be  $63.3 \pm 2.5$  nsec, and those of the 1908- and 2153-keV levels in  $^{200}\text{Pb}$  are  $1.50 \pm 0.08$  and  $47.6 \pm 2.5$  nsec, respectively.

### I. INTRODUCTION

Recent investigations<sup>1-3</sup> of the neutron-deficient isotopes  $^{192-200}\text{Hg}$  have given new information about the lowest collective excitations of these even nuclei and have also revealed new negative-parity levels. The properties of the collective positive-parity states show a remarkable independence of the neutron number and appear to have characteristics midway between those expected for a vibrating spherical nucleus and a rigid rotating spheroidal nucleus. The properties of the

negative-parity states, however, appear to be more dependent on neutron number. This is rather surprising in view of their theoretical description<sup>4,5</sup> as two-proton-hole states coupled to phonon excitations. In order to study further the nuclear level structure in this region, we have extended our investigations to the neutron-deficient Pb isotopes where proton shell closure occurs.

During the course of our experiments, which we have reported in part earlier,<sup>6</sup> we learned of similar investigations by Hanser<sup>7,8</sup> and by Ishihara.<sup>9</sup> The results of these authors appear part-